View metadata, citation and similar papers at core.ac.uk

brought to you by CORE

provided by Elsevier - Publisher Connector

Available online at www.sciencedirect.com

ScienceDirect

International Journal of Solids and Structures 44 (2007) 3218–3230

INTERNATIONAL JOURNAL OF SOLIDS and STRUCTURES

www.elsevier.com/locate/ijsolstr

Morphological instability of two stressed spherical shells

Jérôme Colin *

Laboratoire de Métallurgie Physique, UMR 6630 du CNRS, Université de Poitiers, BP 30179, 86962 Futuroscope Cedex, France

Received 19 January 2006; received in revised form 25 August 2006
Available online 23 September 2006

Abstract

The morphological stability of the external free surface of a composite structure made of two shells stressed through the interface has been investigated when mass rearrangement along the surface is controlled by surface diffusion. Due to epitaxy or thermal change, an eigenstrain located in the inner shell is considered. The resulting stress and strain tensors have been first calculated assuming that the interface between the two initially spherical shells is coherent. The roughness appearing by surface diffusion on the external surface of the structure has been then developed on a basis of complete spherical harmonics and the linear stability of the surface has been investigated with respect to each harmonic $Y_l^m(\theta,\varphi)$. The growth rate of the lth order harmonic has been determined and the influence of the geometric and physical parameters such as the radius of the interface, the radii of the free surfaces, the intrinsic deformation or the surface energy has been characterized. The case of a spherical solid embedded in a finite-size matrix has been also discussed.
© 2006 Elsevier Ltd. All rights reserved.

Keywords: Diffusion, surface; Elastic material; Asymptotic analysis; Instability

1. Introduction

The morphological instability of stressed solids has been widely investigated since it has been observed that the roughness of free surfaces and interfaces can strongly modify the mechanical properties of solids such as multilayers, cubic precipitates in superalloys, pore channels or axi-symmetrical conductors used for a number of technological applications ranging from micro-electronics to aeronautics. The first studies of the linear stability of the free surface of a planar solid non-hydrostatically stressed have been performed by Asaro and Tiller (1972) and co-workers (Spencer et al., 1991; Srolovitz, 1991; Freund and Jonsdottir, 1993; Grilhé, 1993; Nozières, 1993; Spencer et al., 1993). Considering different mass transport mechanisms such as surface diffusion or evaporation/condensation mechanism, it has been demonstrated that the surface is unstable with respect to sinusoidal perturbation of wavelength greater than a critical value depending on the physical parameters of the solids such as the surface energy, the elastic constants or the applied stress. This instability driven by the lowering of the total energy stored in the solid has been found to be independent of the mass

* Tel.: +33 549 496 652; fax: +33 549 496 642.
E-mail address: jerome.colin@univ-poitiers.fr

0020-7683/$ - see front matter © 2006 Elsevier Ltd. All rights reserved.
doi:10.1016/j.ijsolstr.2006.09.019

transport mechanism which only affects the expression of the growth rate of the fluctuation and the critical wavelength. A variational approach has been also developed by Grinfeld (1993) who characterized in the frame of the thermodynamics of heterogeneous systems, the morphological change of solids. Recently, the study of the surface instability in biaxially stressed solids has demonstrated that a new diamond morphology is favored when the stress is tensile in one direction and compressive in the orthogonal one (Berger et al., 2003). The effect of morphological change in self-organized nanowire array in InAs/GaSb superlattices due to interfacial bonds has been also studied (Li et al., 2005) as well as the competition as a strain-relief mechanism between misfit dislocations and stress-induced instability of a growing film/vapor interface in the case of an epitaxially stressed thin film on a substrate (Haataja et al., 2002). It can be noticed that the effect of stress on the directional solidification of a planar solid in an external thermal gradient has been carried out and the non-linear evolution of the roughness has been characterized (Cantat et al., 1998).

The morphological change of a number of materials developing non-planar geometry has been investigated when different conditions of stress are considered. For example, the study of the axi-symmetrical rods evolution by surface diffusion under longitudinal stress has given rise to an extensive literature. Introducing axial and radial sinusoidal fluctuations onto the surface of the cylinder, the conditions of its stability have been characterized (Suo and Wang, 1994; Colin et al., 1997; Wang and Suo, 1997). The case of non-axi-symmetric instability has been also recently investigated (Kirill et al., 1999; Kirill et al., 2002). The analytical study of the linear stability of the surface of solids has been completed by numerical simulations of the evolution of the roughness in the non-linear regime in the case of planar and axi-symmetrical geometries (Chiu and Gao, 1993; Yang and Srolovitz, 1993; Kassner and Misbah, 1994; Spencer and Meiron, 1994; Suo and Wang, 1994; Wang and Suo, 1997). The possibility of formation of cracks from the surface has been discussed and the pinch-off of cylindrical structures has been observed.

The case of a spherical solid has been also investigated. In the field of materials science and metallurgy, one of first studies of the linear stability of a sphere has been performed to the author's knowledge, by Mullins and Sekerka (1963). Assuming that a spherical particle in contact with its melt undergoes diffusion-controlled growth, the development of a perturbation expanded on a basis of spherical harmonics has been analyzed in the linear regime. In particular, the critical radius of the sphere above which the first harmonic Y_2^m breaking the symmetry of the sphere may develop has been determined. The problem of the solidification of the particle by heat flow has been also investigated by the same authors. The evolution of the sphere when mass rearrangement occurs through surface diffusion has been then investigated by Nichols and Mullins (1965) and the effect of capillarity on the development of a spherical harmonic has been investigated. The influence of stress on the development of the fluctuation has been characterized later by Leo et al. (1985) and Leo and Sekerka (1989) in the case of a binary alloy consisting in a growing spherical precipitate embedded in an infinite-size matrix. Assuming that atoms are diffusing in the matrix, the stability of the interface of the epitaxially stressed precipitate has been investigated as a function of the lattice mismatch and shear modulii of both phases. In this frame, numerical simulations have been performed and the Ostwald ripening and coarsening have been characterized (Jou et al., 1997; Leo et al., 2000; Akaiwa et al., 2001; Thornton et al., 2001; Akaiwa et al., 2001; Li et al., 2003). Two and three dimensional calculations have been carried out and the microstructure evolution has been determined as a function of the elastic in-homogeneity, epitaxy or applied fields. It has also to be noticed that the effect of composition stress on the stability of a growing spherical particle in contact with its melt has been studied by Caroli et al. (1989) within the framework of Cahn–Larché formalism of diffusion under stress (Larché and Cahn, 1985).

The problem of the evolution of a spherical void in a 3D solid under stress has been analyzed. Three kinetic processes have been successively considered: surface diffusion, diffusion in a fluid inside the cavity and surface reaction. In the three cases, it is found that the void may evolve from a sphere to a penny-shaped crack (Sun et al., 1994). The effect of a constant strain rate of the loading on the evolution of the void shape has been also analyzed.

In the field of continuum mechanics, the case of a stressed spherical shell has been investigated (Wesolowski, 1967; Wang and Ertepinar, 1972; Ogden, 1984). Considering internally or externally pressurized shells, a bifurcation analysis has been carried out for neo-Hookean materials and the critical strain above which shape instability and buckling occur has been determined. The different unstable modes have been found to depend on the strain-energy function and on the thickness of the shells. Recently, the effect of volumetric growth in the

stability of biological tissues modelled by hyperelastic materials in the theory of finite elasticity has been studied (Ben-Amar and Goriely, 2005). The role of mechanical and geometric effects have been identified.

In this paper, the stability of the external free surface of a composite shell made of two spherical shells under stress with a coherent interface is studied assuming that the mass transport mechanism is surface diffusion. Within linear and isotropic elasticity theory, the effect of stress on the development of a fluctuation described by a spherical harmonic is characterized. In the linear regime, the effect of geometric and mechanical parameters such as the different radii or the eigenstrain are investigated.

2. Formulation of the problem

A composite spherical shell is made of two shells, the inner and outer radii are respectively labelled R_1 and R for the first shell and R and R_2 for the second one (see Fig. 1). Using spherical coordinates (r, θ, φ), the interface between the two shells is located at $r = R$. It is assumed that the elastic constants are equal in both shells, the Young modulus is labelled μ and Poisson's ratio ν. The interface between the two solids is coherent and a constant eigenstrain ϵ^* is introduced (without loss of generality) in the first shell, i.e., for $R_1 \leqslant r \leqslant R$, $E^{1,(*)}_{rr}(r) = E^{1,(*)}_{\theta\theta}(r) = E^{1,(*)}_{\varphi\varphi}(r) = \epsilon^*$. The origin of the eigenstrain or intrinsic deformation may be for example the lattice mismatch between the two crystalline substances of different lattice parameters when the shells are epitaxially stressed or the mismatch between thermal expansion coefficients in the case of thermally stressed shells. The stability results of the structure obtained in this paper can also be generalized to pressurized shells.

2.1. Determination of stress and strain tensors in the initially spherical shells

In both phases, the initial stress and total strain tensors respectively labelled $T^{k,(0)}$ and $E^{k,(0)}$ are defined as follows:

$$T^{k,(0)} = \mathbb{C}^k\left(E^{k,(0)} - E^{k,(*)}\right), \tag{1}$$

with $k = 1, 2$ in the first and second shell respectively. $\mathbb{C}^k$ is the elastic constant tensor and $E^{k,(*)}$ is the eigenstrain tensor already defined:

$$E^{1,(*)} = \epsilon^* \mathscr{I}, \quad E^{2,(*)} = 0, \tag{2}$$

where $\mathscr{I}$ is the unit tensor. The stress $T^{k,(0)}$ must also satisfy to the Cauchy's equation in both phases:

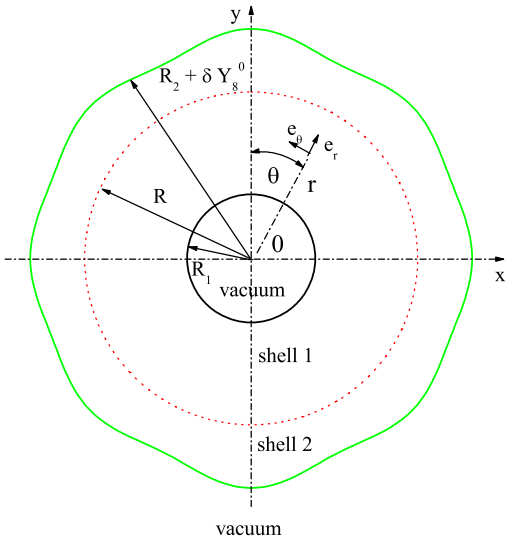

Fig. 1. The external radius of the second shell is perturbed by the spherical harmonic $Y^0_8(\theta, \varphi)$.

$$\nabla \cdot T^{k,(0)} = 0, \tag{3}$$

characterizing the mechanical equilibrium in the bulk. Introducing Eq. (1) into Eq. (3) leads to the following modified Navier's equation for the displacement field $\tilde{u}^{k,(0)}$:

$$\nabla^2 \tilde{u}^{k,(0)} + \frac{1}{1-2v}\nabla\left(\nabla \cdot \tilde{u}^{k,(0)}\right) = \frac{2(1+v)}{1-2v}\nabla E^{k,(*)}. \tag{4}$$

The above Eq. (4) is equivalent to the bulk equilibrium equation derived in the case of thermo-elastic problems (Boley and Weiner, 1960) with an eigenstrain $E^{k,(*)}$ defined as the thermal expansion coefficient times the temperature. In the case of a coherent interface, two supplementary boundary conditions have to be satisfied. Neglecting the capillarity stress, the equilibrium of forces onto the interface writes:

$$\left(T^{1,(0)} - T^{2,(0)}\right)\tilde{n} = \tilde{0}, \tag{5}$$

where $\tilde{n}$ is the normal to the interface pointing into the second shell. The continuity of total displacement $\tilde{u}^{k,(0)}$ writes:

$$\tilde{u}^{1,(0)} = \tilde{u}^{2,(0)}. \tag{6}$$

The mechanical equilibrium of both free surfaces leads to the following equations:

$$T^{1,(0)}\tilde{n}^1 = \tilde{0}, \quad \text{for} \quad r = R_1 \tag{7}$$

and

$$T^{2,(0)}\tilde{n}^2 = \tilde{0}, \quad \text{for} \quad r = R_2 \tag{8}$$

with $\tilde{n}^1$ and $\tilde{n}^2$ two outer normal vectors to the surfaces located at $r = R_1$ and $r = R_2$, respectively. Since the intrinsic deformation of the shells is assumed to be symmetric with respect to the origin, the general expression of the displacement is $\tilde{u}^{k,(0)}(\tilde{r}) = u_r^{k,(0)}(r)\ \tilde{e}_r$, with $\tilde{e}_r$ the radial unit vector. Navier's equation (4) is then satisfied for a radial displacement $u_r^{k,(0)}$ given by (Boley and Weiner (1960)):

$$u_r^{k,(0)}(r) = A_k^0 r + \frac{B_k^0}{r^2} + \frac{1+v}{1-v}\frac{1}{r^2}\int_{r_*}^{r} E^{k,(*)}(r')r'^2 \mathrm{d}r', \tag{9}$$

where r_*, A_k^0 and B_k^0 are constants to be specified. Using the classical definition of strain tensor $E_{kl}^{i,(0)} = 1/2(\partial u_k^{i,(0)}/\partial x_l + \partial u_l^{i,(0)}/\partial x_k)$ and Hooke's law, the strain and stress tensors can easily be derived as a function of the constants A_k^0 and B_k^0 (Boley and Weiner, 1960). For example the radial component of stress $T_{rr}^{k,(0)}$ is given by

$$T_{rr}^{k,(0)}(r) = 2\mu\frac{1+v}{1-2v}A_k^0 - 4\mu\frac{B_k^0}{r^3} - 4\mu\frac{1+v}{1-v}\frac{1}{r^3}\int_{r_*}^{r} E^{k,(*)}(r')r'^2 \mathrm{d}r'. \tag{10}$$

A similar relation holds for the "hoop" stress $T_{\theta\theta}^{k,(0)} = T_{\varphi\varphi}^{k,(0)}$ (see Appendix). Taking $r^* = R_1$ in the definition of displacement and stress Eqs. (9) and (10), the equilibrium Eqs. (5)–(8) have been used to determine the four constants A_k^0 and B_k^0 (with $k = 1,2$) characterizing the elastic state of the two shells (see Appendix). The two components of stress $T_{rr}^{2,(0)}$ and $T_{\theta\theta}^{2,(0)}$ which participate to the destabilization of the external free surface have been found to be:

$$T_{rr}^{2,(0)}(r) = 4\mu\frac{1+v}{1-v}\epsilon^*\frac{R^3 - R_1^3}{R_2^3 - R_1^3}\frac{r^3 - R_2^3}{3r^3}, \tag{11}$$

$$T_{\theta\theta}^{2,(0)}(r) = 2\mu\frac{1+v}{1-v}\epsilon^*\frac{R^3 - R_1^3}{R_2^3 - R_1^3}\frac{2r^3 + R_2^3}{3r^3}. \tag{12}$$

It can be noticed that the initial stress tensor is such that $T_{\theta\theta}^{k,(0)} = T_{\varphi\varphi}^{k,(0)}$. This relatively simple form of initial stress allows for solving analytically the elasticity problem of the perturbed shells in the next section using Leo et al. (1985) results.

2.2. Kinetics of the external surface

The evolution of the external free surface of the structure is assumed to be controlled by surface diffusion. It is well admitted (Asaro and Tiller, 1972; Larché and Cahn, 1985; Spencer et al., 1991; Chiu and Gao, 1993; Yang and Srolovitz, 1993; Suo and Wang, 1994) that the chemical potential of a stressed solid undergoing morphological change by surface diffusion is defined by $\mu_c = \Omega(\gamma\ \kappa + G^{elas})$, where Ω is the atomic volume, γ the surface energy, κ the curvature of the surface in the reference state and G^{elas} the elastic energy density at the surface. The resulting surface flux of atoms is defined by (Mullins, 1957; Larché and Cahn, 1985):

$$\widetilde{J}_S = -\frac{D_S\zeta}{kT}\nabla_S\mu_c = -\frac{D_S\zeta\Omega}{kT}\nabla_S\left(\gamma\kappa + G^{elas}\right), \tag{13}$$

where ∇_S is the surface gradient, D_S the surface diffusivity of atoms, k Boltzmann's constant, T the temperature, ζ the number of atoms per unit area. The motion of the surface is then controlled by the accumulation of diffusing atoms (Spencer et al., 1991):

$$\frac{\partial\tilde{r}}{\partial t} = -\Omega(\nabla_S\cdot\widetilde{J}_S)\tilde{n}^2, \tag{14}$$

and the normal component of Eq. (14) gives the non-linear evolution equation of the external free surface:

$$\frac{\partial\rho}{\partial t} = \frac{D_S\Omega^2\zeta\gamma}{kT}\left(1+|\nabla\rho|^2\right)^{1/2}\nabla_S^2\left(\kappa + \frac{G^{elas}}{\gamma}\right), \tag{15}$$

with ∇_S^2 the surface Laplacian. At each step of the evolution of the surface profile, the elasticity Eqs. (5)–(8) have to be solved and the elastic energy density has to be evaluated at the surface. The profile of the surface is then evolved according to the time evolution Eq. (15). It is assumed that the time scale for elastic deformation is small compared to the time scale of diffusion of atoms. In the next section, a fluctuation has been introduced on the external surface of the structure and the coupled equations of elasticity and diffusion have been solved to the first order in amplitude of the perturbation. The growth rate of the fluctuation has been then determined and the early beginning of its evolution has been characterized in the linear regime.

3. Morphological instability of the structure

The external radius of the shell $\rho(\theta,\varphi,t)$ is perturbed with the help of the complete spherical harmonic $Y_l^m(\theta,\varphi)$:

$$\rho(\theta,\varphi,t) = R_2 + \delta(t)Y_l^m(\theta,\varphi) = R_2\left(1+\delta_*(t)Y_l^m(\theta,\varphi)\right), \tag{16}$$

where $\delta(t)$ is the amplitude of the perturbation, t the time and $\delta_* = \delta/R_2 \ll 1$ the corresponding small dimensionless parameter used for the perturbation development. To the first order in δ_*, the displacement, strain and stress write:

$$\begin{aligned}
\tilde{u}^k &= \tilde{u}^{k,(0)} + \delta_*\tilde{u}^{k,(1)} + \Theta(\delta_*^2),\\
E_{ij}^k &= E_{ij}^{k,(0)} + \delta_* E_{ij}^{k,(1)} + \Theta(\delta_*^2),\\
T_{ij}^k &= T_{ij}^{k,(0)} + \delta_* T_{ij}^{k,(1)} + \Theta(\delta_*^2).
\end{aligned} \tag{17}$$

Navier's Eq. (4) is then re-written as:

$$\nabla^2\tilde{u}^{k,(1)} + \frac{1}{1-2v}\nabla\left(\nabla\cdot\tilde{u}^{k,(1)}\right) = 0. \tag{18}$$

Following Leo et al. (1985) and Caroli et al. (1989) the perturbed displacement $\tilde{u}^{k,(1)}$ can be taken of the form:

$$
\begin{aligned}
u_r^{k,(1)}(r,\theta,\varphi) &= f_k(r) Y_l^m(\theta,\varphi),\\
u_\theta^{k,(1)}(r,\theta,\varphi) &= g_k(r)\frac{\partial Y_l^m}{\partial\theta}(\theta,\varphi),\\
u_\varphi^{k,(1)}(r,\theta,\varphi) &= h_k(r)\frac{1}{\sin\theta}\frac{\partial Y_l^m}{\partial\varphi}(\theta,\varphi),
\end{aligned}
\tag{19}
$$

where the functions f_k, g_k and h_k are defined by

$$
\begin{aligned}
f_k(r) &= A_k^1 r^{l-1} + B_k^1 r^{l+1} + C_k^1 r^{-l-2} + D_k^1 r^{-l},\\
g_k(r) &= \frac{1}{l}A_k^1 r^{l-1} + \zeta B_k^1 r^{l+1} - \frac{1}{l+1}C_k^1 r^{-l-2} + \varsigma D_k^1 r^{-l},\\
h_k(r) &= g_k(r),
\end{aligned}
\tag{20}
$$

with the constants A_k^1, B_k^1, C_k^1 and D_k^1 to be determined. The coefficients ζ and ς are defined as follow:

$$
\zeta = \frac{l+5-4\nu}{(l+1)(l-2+4\nu)}, \quad \varsigma = \frac{4-l-4\nu}{l(l+3-4\nu)}. \tag{21}
$$

The normal to the external perturbed surface is also modified as $\tilde{n}^2 = (1, -\delta_* \frac{\partial Y_l^m}{\partial\theta}, -\frac{\delta_*}{\sin\theta}\frac{\partial Y_l^m}{\partial\varphi})$. Since the elastic coefficients are assumed equal in both shells, the elastic relaxation is completely determined by only one displacement field in the shells $\tilde{u}^{1,(1)} = \tilde{u}^{2,(1)} = \tilde{u}^{(1)}$ with four constants A^1, B^1, C^1, D^1. The stress and strain tensors of relaxation are respectively labelled $T^{(1)}$ and $E^{(1)}$ and the boundary conditions write:

$$
\left(T^{2,(0)} + \delta_* T^{(1)}\right)\tilde{n}^2 = \tilde{0}, \quad \text{for} \quad r = \rho, \tag{22}
$$

$$
\left(T^{1,(0)} + \delta_* T^{(1)}\right)\tilde{n}^1 = \tilde{0}, \quad \text{for} \quad r = R_1. \tag{23}
$$

The development of the above system to the first order in δ_* leads to:

$$
T_{rr}^{(1)}(r=R_2) = -\left.\frac{\partial T_{rr}^{2,(0)}}{\partial r}\right|_{r=R_2} R_2 Y_l^m(\theta,\varphi), \tag{24}
$$

$$
T_{r\theta}^{(1)}(r=R_2) = T_{\theta\theta}^{2,(0)}(r=R_2)\frac{\partial Y_l^m}{\partial\theta}, \tag{25}
$$

$$
T_{r\varphi}^{(1)}(r=R_2) = T_{\varphi\varphi}^{2,(0)}(r=R_2)\frac{1}{\sin\theta}\frac{\partial Y_l^m}{\partial\varphi}, \tag{26}
$$

$$
T_{rr}^{(1)}(r=R_1) = 0, \tag{27}
$$

$$
T_{r\theta}^{(1)}(r=R_1) = 0, \tag{28}
$$

$$
T_{r\varphi}^{(1)}(r=R_1) = 0. \tag{29}
$$

It can be noticed that in the hypothesis where $T_{\theta\theta}^{k,(0)} = T_{\varphi\varphi}^{k,(0)}$ the Eqs. (25), (26) and (28), (29) are degenerated and the system reduces to four independent equations that have been used to determine the four constants A^1, B^1, C^1, D^1 (see Appendix). The elastic energy density at the external surface $G^{\text{elas}} = \frac{1}{2}\left(T_{ij}^{2,(0)} + \delta_* T_{ij}^{(1)}\right)\left(E_{ij}^{2,(0)} + \delta_* E_{ij}^{(1)}\right)$ has been then developed to the first order in δ_*:

$$
G^{\text{elas}} = g_0^{\text{elas}} + \delta_* g_1^{\text{elas}} + \Theta(\delta_*^2), \tag{30}
$$

with

$$
g_0^{\text{elas}} = \frac{1}{2}T_{ij}^{2,(0)}(r=R_2)E_{ij}^{2,(0)}(r=R_2), \tag{31}
$$

$$
\begin{aligned}
g_1^{\text{elas}} = {} & \frac{1}{2}T_{ij}^{2,(0)}(r=R_2)\left.\frac{\partial E_{ij}^{2,(0)}}{\partial r}\right|_{r=R_2} R_2 Y_l^m(\theta,\varphi) + \frac{1}{2}\left.\frac{\partial T_{ij}^{2,(0)}}{\partial r}\right|_{r=R_2} E_{ij}^{2,(0)}(r=R_2) R_2 Y_l^m(\theta,\varphi)\\
& + T_{ij}^{2,(0)}(r=R_2)E_{ij}^{(1)}(r=R_2).
\end{aligned}
\tag{32}
$$

The time evolution Eq. (15) of the perturbation amplitude δ finally reads:

$$\frac{1}{\delta}\frac{\mathrm{d}\delta}{\mathrm{d}t}=\frac{D_S\Omega^2\zeta\gamma}{kTR_2^4}l(l+1)\left[-(l-1)(l+2)+\frac{R_2}{R_*}\frac{\left(R^3-R_1^3\right)^2}{\left(R_2^3-R_1^3\right)^2}f(R_1,R_2,l,v)\right], \tag{33}$$

where $R_*=\mu\gamma/T_0^2$ and $T_0=2\mu\frac{1+v}{1-v}\epsilon^*$ are respectively the characteristic length and stress of the problem. The dimensionless function f is defined by

$$f(R_1,R_2,l,v)=1+\frac{f_1(R_1,R_2,l,v)}{f_2(R_1,R_2,l,v)}, \tag{34}$$

with

$$\begin{aligned}f_1(R_1,R_2,l,v)=&(2l+1)^2((2v-1)l^4+(4v-2)l^3+(-4v^2+6v-3)l^2+(-4v^2+4v-2)l-8(2v^2\\&-3v+1))R_2^{2l+4}R_1^{2l}-2l(4l^5+12l^4+l^3-18l^2-5l+6)vR_2^{2l+2}R_1^{2l+2}+(2l+1)^2(l^4\\&+2l^3-l^2-2l-4v^2+4)R_2^{2l}R_1^{2l+4}+2(2(v-1)l^5+(4v^2-5v-1)l^4-4(v^2-v\\&+1)l^3+(7v^2-v-4)l^2+(9v^2-5)l+2(v^2-1))R_2R_1^{4l+3}-2(2(v-1)l^5+(-4v^2\\&+15v-9)l^4-4(5v^2-11v+5)l^3+(-43v^2+63v-22)l^2+(-33v^2+44v-15)l\\&-8v^2+12v-4)R_2^{4l+3}R_1,\end{aligned} \tag{35}$$

and

$$\begin{aligned}f_2(R_1,R_2,l,v)=&-(2l+1)^2(l^4+2l^3-l^2-2l-4v^2+4)R_2^{2l+4}R_1^{2l}+2l(4l^5+12l^4+l^3-18l^2-5l\\&+6)R_2^{2l+2}R_1^{2l+2}-(2l+1)^2(l^4+2l^3-l^2-2l-4v^2+4)R_2^{2l}R_1^{2l+4}\\&+4(l^4+2l^3+(3-4v^2)l^2+(2-4v^2)l-v^2+1)R_2R_1^{4l+3}+4(l^4+2l^3+(3-4v^2)l^2\\&+(2-4v^2)l-v^2+1)R_2^{4l+3}R_1.\end{aligned} \tag{36}$$

The time evolution of the fluctuation amplitude δ has been found to be:

$$\delta(t)=\delta(0)\exp\left[\frac{\tau}{\tau_0}t\right], \tag{37}$$

with the dimensionless growth rate τ:

$$\tau=l(l+1)\left[-(l-1)(l+2)+\frac{R_2}{R_*}\frac{(R^3-R_1^3)^2}{(R_2^3-R_1^3)^2}f(R_1,R_2,l,v)\right], \tag{38}$$

and the constant $\tau_0=kTR_2^4/D_S\Omega^2\zeta\gamma$. The first capillarity term in Eq. (38) is negative and favors the decay of the perturbation, the second term coming from elasticity is positive and favors its growth. It can be observed from Eqs. (35), (36) and (38) that in the general case of two shells of finite thickness, the growth rate τ does not depend on m but depends in a non-trivial form on the different radii R_1, R_2 and R. In a first time, the stability of the external surface has been studied in the interesting limit case of a spherical precipitate embedded in a finite size matrix. Taking $R_1=0$ in Eq. (38), the growth rate simplifies as follow:

$$\tau=-l(l+1)(l+2)\left[l-1-\frac{(2l^2+5l+3)(1-v)}{2(l^2+(1+2v)l+1+v)}\frac{R^5}{R_2^5}\frac{R}{R_*}\right]. \tag{39}$$

Since when $l=1$ the fluctuation does not break the symmetry of the structure, the first perturbation for which the shape of the shell is modified is Y_2^m. From Eq. (39), the condition $\tau(l=2)=0$ allows for determining the critical external radius below which at least the second harmonic Y_2^m may develop:

$$R_2\leqslant R_2^c(2)=\left[\frac{21(1-v)}{2(7+5v)}\frac{R}{R_*}\right]^{1/5}R. \tag{40}$$

For the lth order harmonic Y_l^m (with $l\geqslant 2$), a critical radius can be also derived, setting $\tau=0$:

$$R_2^c(l) = R_2^c(2)\left[\frac{(7+5\nu)(2l^2+5l+3)}{21(l-1)(l^2+(1+2\nu)l+1+\nu)}\right]^{1/5} \leqslant R_2^c(2). \tag{41}$$

It can be observed in Eq. (40) that the first critical radius $R_2^c(2)$ only depends on the physical parameters of the shells through the R_* radius. As the eigenstrain ϵ^* increases, this critical radius below which the second harmonic starts to growth increases. It demonstrates the destabilizing effect of stress on the external surface: an initially stable shell may become unstable as soon as due to a sufficiently high value of the intrinsic deformation, its external radius becomes smaller than the critical radius. From Eq. (41), it can be first noticed that once $R_2^c(2)$ is defined, the ratio $R_2^c(l)/R_2^c(2)$ only depends on l and ν. For given values of the radius R of the precipitate and of the eigenstrain ϵ^*, the critical radius below which the lth order harmonic may appear decreases as l increases. This can be explained since for high order harmonics ($l \gg 2$) and for given values of the radii R_2, R, R_*, the capillarity term $\gamma\kappa$ and the elastic energy density g_1^{elas} introduced in Eq. (33) grow like $\sim l^2$ and $\sim l$, respectively. In that case (taking $l \to +\infty$), it yields:

$$R_2^c(l) \sim \left(\frac{1-\nu}{l}\frac{R}{R_*}\right)^{1/5} R. \tag{42}$$

Once R and R_* are given, the maximum number of harmonics susceptible to develop is theoretically limited by the following geometric condition, $R_2^c(l) \geqslant R$ leading to:

$$\frac{R}{R_*} \geqslant \frac{2(l-1)}{1-\nu}\frac{l^2+l(1+2\nu)+1+\nu}{2l^2+5l+3}. \tag{43}$$

When R approaches infinity, the problem reduces to the study of the morphological instability of a semi-infinite planar solid under stress T_0. The growth rate of a sinusoidal perturbation of the free surface appearing by surface diffusion can be for example derived from Eqs. (37) and (39). One takes $R_2 = R$ such that the eigenstrain spreads out in all the solid and $\lambda \sim 2\pi R/l$ with $\lambda = 2\pi/k$ the average wavelength of the sinusoidal fluctuation and k the corresponding wavenumber (Mullins and Sekerka, 1963). Re-scaling the constant τ_0 in Eq. (37) to $\tau_0 = kT/D_S\Omega^2\zeta\gamma$, the growth rate of the fluctuation writes:

$$\tau \sim k^3 k_c - k^4, \tag{44}$$

with the critical wavenumber $k_c = (1-\nu)T_0^2/\mu\gamma$. The well-known results obtained in the planar case (Asaro and Tiller, 1972; Spencer et al., 1991; Srolovitz, 1991; Grinfeld, 1993) can be easily derived from Eq. (44): the free surface of the planar solid is unstable with respect to fluctuation of wavenumber $k \leqslant k_c$. The wavenumber selected by diffusion such that the growth rate in Eq. (44) is maximum is $k = 3/4k_c$.

The general case of two shells of finite radii can be now investigated. In the case of an aluminum structure, the growth rate τ of the fluctuation Y_l^m has been plotted in Fig. 2 as a function of l for increasing values of the

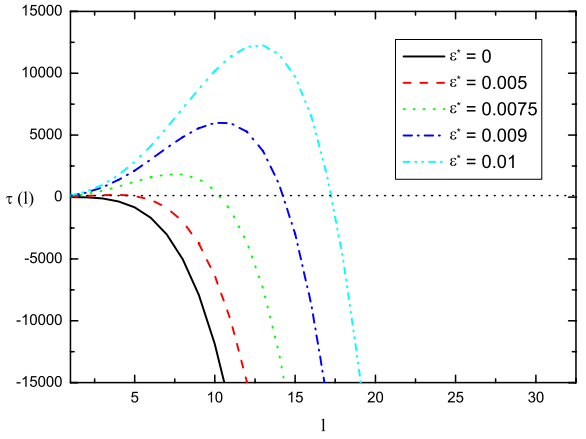

Fig. 2. Growth rate τ versus l for different values of the eigenstrain ϵ^*.

eigenstrain and for the given radii $R_2 = 4\ \mu m$, $R = 3\ \mu m$, $R_1 = 1\ \mu m$, $R_* = 2.9281610^{-6}/\epsilon_*^2\ \mu m$. The values of the different physical parameters are taken as follow: $\mu = 26$ GPa, $\nu = 0.33$, $\gamma \approx 1.2$ J m^{-2} (Schöchlin et al., 1995). It can be observed that as ϵ^* increases, the number of harmonics for which the growth rate is positive increases leading to the development of a rough surface. The critical radii $R_2^c(2)$ and $R_2^c(3)$ below which the second and third harmonics Y_2^m and Y_3^m respectively may appear have been then plotted in Fig. 3 as a function of the inner radius of the first shell R_1, for a constant eigenstrain $\epsilon^* = 0.01$ and for a radius of the interface given by $R = 3\ \mu m$. It can be noticed that these two critical radii slowly decrease until $R_1 \approx 1/3R = 1\ \mu m$ and then strongly decrease. It can be concluded at this point that at constant eigenstrain, the development of the first two harmonics on the external surface is facilitated when the first shell is thick, the most favorable case being the spherical precipitate embedded in a matrix already studied. Although the geometry and the condition of stress are different from the case already studied by Sun et al. (1994) which consists in a spherical void in a 3D solid under stress, the development of the Y_2^0 harmonic confirms that a spherical structure can be unstable and may evolve to a spheroid. For a very thin inner shell of radii R_1 and R, the eigenstrain has to be increased to facilitate the development of the roughness on the external surface. In the case of two very thin shells of equal thickness, taking $R_2 = R + \Delta/2$ and $R_1 = R - \Delta/2$ with $\Delta/R \ll 1$, the growth rate defined in Eq. (38) can be expanded in power of Δ:

$$\tau = -\left[(l-1)(l+2) - \frac{(1-\nu)}{4(1+\nu)}\frac{R^2}{R_*\Delta} - \frac{(l^2+l+2)(1-\nu)}{8(1+\nu)}\frac{R}{R_*} - \frac{(1+2\nu)l^4+2(1+2\nu)l^3}{48(1+\nu)^2}\frac{\Delta}{R_*} + \frac{(5\nu^2+2\nu-4)l^2+(5\nu^2+4\nu-3)l-4\nu^2+4}{48(1+\nu)^2}\frac{\Delta}{R_*}\right] l(l+1) + \Theta(\Delta^2), \tag{45}$$

and the critical radius $R_2^c(l)$ has been found to be:

$$R_2^c(l) = R + \frac{1}{2}\frac{a - \frac{1}{2}\sqrt{b}}{c}, \tag{46}$$

with

$$\begin{aligned} a &= 3R\nu^2l^2 + 24R_*\nu^2l^2 - 3Rl^2 + 24R_*l^2 + 48R_*\nu l^2 + 3R\nu^2l + 24R_*\nu^2l - 3Rl + 24R_*l \\ &\quad + 48R_*\nu l + 6R\nu^2 - 48R_*\nu^2 - 6R - 48R_* - 96R_*\nu, \\ b &= 48(\nu^2-1)((2\nu+1)l^4 + (4\nu+2)l^3 + (-5\nu^2-2\nu+4)l^2 + (-5\nu^2-4\nu+3)l \\ &\quad + 4(\nu^2-1))R^2 + 36(\nu+1)^2((l^2+l+2)R(\nu-1) + 8(l^2+l-2)R_*(\nu+1))^2, \qquad (47) \\ c &= (2\nu+1)l^4 + (4\nu+2)l^3 + (-5\nu^2-2\nu+4)l^2 + (-5\nu^2-4\nu+3)l + 4(\nu^2-1). \qquad (48) \end{aligned}$$

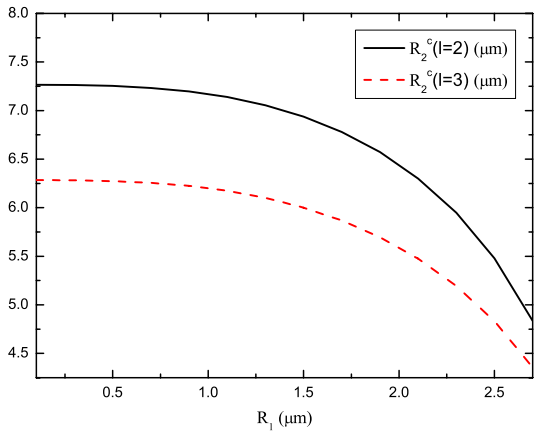

Fig. 3. Critical radii $R_2^c(2)$ and $R_2^c(3)$ versus R_1 for $\epsilon^* = 0.01$ and $R = 3\ \mu m$.

This above expression of the critical value of the external radius holds for thin shells with a small eigenstrain ϵ^*. Considering the numerical values of the physical parameters used in this paper, it corresponds to an eigenstrain smaller than 0.15%. Finally, the variation of the two characteristic modes l_c and l_p can be numerically determined in the general case of two shells of finite thickness. The critical mode l_c defined by $\tau = 0$ is such that for $l \leqslant l_c$, $\tau \geqslant 0$ and the corresponding harmonic may develop. Among all the possible harmonics, one is assumed to be favored by surface diffusion and is assumed to develop faster than the others, this mode is defined by:

$$\left.\frac{\partial \tau}{\partial l}\right|_{l=l_p} = 0. \tag{49}$$

The modes l_c and l_p have been plotted as a function of R_1 for $\epsilon^* = 0.01$ in Fig. 4(a) and versus ϵ^* for $R_1 = 1$ μm in Fig. 4(b). It can be observed in Fig. 4(a) that both critical and most probable modes l_c and l_p are almost constant until $R_1 \approx 1$ μm. For $R_1 > 1$ μm, they decrease as the thickness of the first shell is reduced. In the case, where the eigenstrain ϵ^* is increased at constant radii (Fig. 4(b)), the values of the modes l_c and l_p increase demonstrating again the destabilizing effect of the stress. It can finally be concluded that a great number of harmonics may develop onto the external surface of the structure depending on the relative values of the inner radius R_1 and of the eigenstrain ϵ^*. The probability that this surface develops a rough profile is increased when the intrinsic deformation takes high values and the inner radius R_1 is small.

4. Conclusion

The linear stability of the external surface of a composite structure made of two stressed spherical shells has been investigated when a fluctuation described by a complete spherical harmonic is assumed to appear by sur-

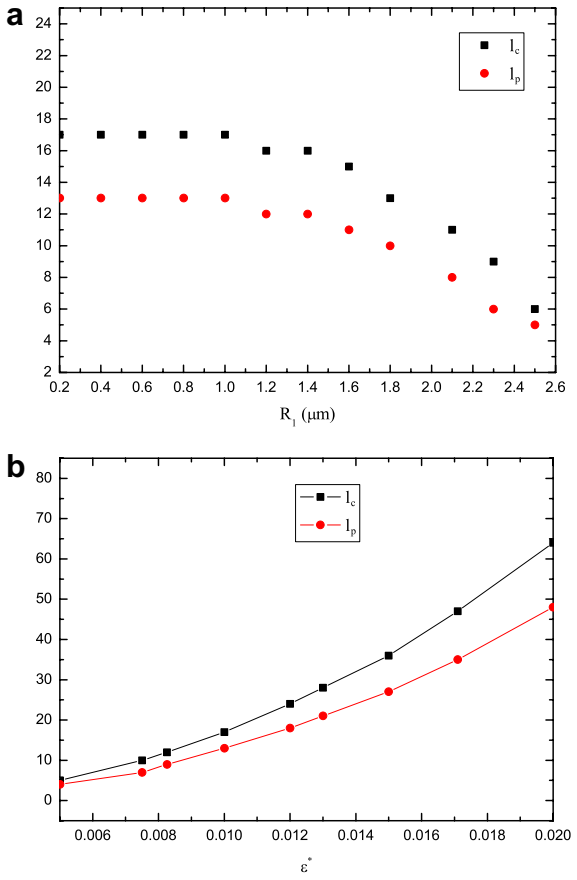

Fig. 4. (a) l_c and l_p versus R_1 for $\epsilon^* = 0.01$ and $R = 3$ μm. (b) l_c and l_p versus ϵ^* for $R_1 = 1$ μm and $R = 3$ μm.

face diffusion on the surface. The growth rate of the amplitude of the perturbation has been determined as a function of different geometric and physical parameters. In the general case of two shells of finite thickness, the growth rate has been plotted versus l modes for increasing values of the eigenstrain. It has been observed that the number of harmonics susceptible to develop increases with the intrinsic deformation leading to a possible rough surface. The effect of the inner radius of the first shell has been then characterized on the critical and most probable modes as well as on the critical radius $R_2^c(2)$ below which the first harmonic Y_2^m that breaks the symmetry develops. In the limit case of a stressed spherical precipitate in the matrix, an analytical expression for the critical external radius below which the lth mode may appear has been determined. In the case of two very thin shells of equal thickness, the critical radius $R_2^c(2)$ has been also estimated. Finally, it can be concluded that the inner radius and eigenstrain are two relevant parameters in the study of the roughness. Their values determine the number of harmonics that may appear for given external radius R_2 and interface R of a given material. In the case where several harmonics may appear, a numerical analysis of the non-linear evolution of the surface taking into account the interaction between these harmonics would be interesting to carry out to get relevant information on the long-time evolution of the amplitude of the roughness.

Finally, it can be underlined that this study may apply to a number of structures ranging from the mesoscopic to the macroscopic scale. For example in the nuclear industry, the new generation of nuclear fuel is made of spherical particles consisting in a core of nuclear materials coated with others materials. Under irradiation, a stress field appears due to nuclear reactions in the bullets leading to the morphological change and ageing of the spent fuel. The present analysis may give some information on the different radii for which the surface instability is supposed to appear.

Appendix A. Elastic solution for the spherical shells

In the case of symmetrical intrinsic deformation of the shells with respect to the origin, the solution to Navier's equation (Boley and Weiner, 1960):

$$\nabla^2 \tilde{u}^{k,(0)} + \frac{1}{1-2v}\nabla\left(\nabla \cdot \tilde{u}^{k,(0)}\right) = \frac{2(1+v)}{1-2v}\nabla E^{k,(*)}. \tag{50}$$

is $\tilde{u}^{k,(0)}(\tilde{r}) = u_r^{k,(0)}(r)\tilde{e}_r$ with

$$u_r^{k,(0)}(r) = A_k^0 r + \frac{B_k^0}{r^2} + \frac{1+v}{1-v}\frac{1}{r^2}\int_{r_*}^{r} E^{k,(*)}(r')r'^2 \mathrm{d}r'. \tag{51}$$

The strain tensor is then defined by:

$$E_{rr}^{k,(0)}(r) = A_k^0 - 2\frac{B_k^0}{r^3} + \frac{1+v}{1-v}E^{k,(*)}(r) - 2\frac{1+v}{1-v}\frac{1}{r^3}\int_{r_*}^{r} E^{k,(*)}(r')r'^2 \mathrm{d}r', \tag{52}$$

$$E_{\theta\theta}^{k,(0)}(r) = E_{\varphi\varphi}^{k,(0)}(r) = A_k^0 + \frac{B_k^0}{r^3} + \frac{1+v}{1-v}\frac{1}{r^3}\int_{r_*}^{r} E^{k,(*)}(r')r'^2 \mathrm{d}r'. \tag{53}$$

The radial stress is given by:

$$T_{rr}^{k,(0)}(r) = 2\mu\frac{1+v}{1-2v}A_k^0 - 4\mu\frac{B_k^0}{r^3} - 4\mu\frac{1+v}{1-v}\frac{1}{r^3}\int_{r_*}^{r} E^{k,(*)}(r')r'^2 \mathrm{d}r', \tag{54}$$

and the "Hoop" stress writes:

$$T_{\theta\theta}^{k,(0)}(r) = T_{\varphi\varphi}^{k,(0)}(r) = 2\mu\frac{1+v}{1-2v}A_k^0 - 2\mu\frac{1+v}{1-v}E^{k,(*)}(r) + 2\mu\frac{B_k^0}{r^3} + 2\mu\frac{1+v}{1-v}\frac{1}{r^3}\int_{r_*}^{r} E^{k,(*)}(r')r'^2 \mathrm{d}r'. \tag{55}$$

Solving the system of equilibrium Eqs. (5)–(8) with $r^* = R_1$, the four constants A_1^0, B_1^0, A_2^0 and B_2^0 have been found to be:

$$A_1^0 = A_2^0 = \frac{2\epsilon^*(1-2\nu)}{3(1-\nu)}\frac{(R^3-R_1^3)}{(R_2^3-R_1^3)}, \tag{56}$$

$$B_1^0 = \frac{\epsilon^*(1+\nu)}{3(1-\nu)}\frac{R_1^3(R^3-R_1^3)}{(R_2^3-R_1^3)}, \tag{57}$$

$$B_2^0 = \frac{\epsilon^*(1+\nu)}{3(1-\nu)}\frac{R_2^3(R^3-R_1^3)}{(R_2^3-R_1^3)}. \tag{58}$$

Appendix B. Elastic solution for the perturbed shells

When the external surface is perturbed by a spherical harmonic, the general form of the displacement field satisfying to Navier's Eq. (18) has already been determined by Leo et al. (1985) and Leo and Sekerka (1989):

$$\begin{aligned} u_r^{(1)}(r,\theta,\varphi) &= f(r)Y_l^m(\theta,\varphi),\\ u_\theta^{(1)}(r,\theta,\varphi) &= g(r)\frac{\partial Y_l^m}{\partial\theta}(\theta,\varphi),\\ u_\varphi^{(1)}(r,\theta,\varphi) &= g(r)\frac{1}{\sin\theta}\frac{\partial Y_l^m}{\partial\varphi}(\theta,\varphi), \end{aligned} \tag{59}$$

with

$$\begin{aligned} f(r) &= A^1 r^{l-1} + B^1 r^{l+1} + C^1 r^{-l-2} + D^1 r^{-l},\\ g(r) &= \frac{1}{l}A^1 r^{l-1} + \zeta B^1 r^{l+1} - \frac{1}{l+1}C^1 r^{-l-2} + \varsigma D^1 r^{-l}, \end{aligned} \tag{60}$$

and

$$\zeta = \frac{l+5-4\nu}{(l+1)(l-2+4\nu)}, \quad \varsigma = \frac{4-l-4\nu}{l(l+3-4\nu)}. \tag{61}$$

The constants A^1, B^1, C^1 and D^1 which are not given in this paper are determined with the help of equilibrium Eqs. (22) and (23). The resulting strain tensor can then easily be derived using the following relations:

$$E_{rr}^{(1)} = \frac{\partial f(r)}{\partial r}Y_l^m(\theta,\varphi), \tag{62}$$

$$E_{\theta\theta}^{(1)} = \left[\frac{f(r)}{r} + \frac{m^2}{\sin^2\theta}\frac{g(r)}{r} - l(l+1)\frac{g(r)}{r}\right]Y_l^m(\theta,\varphi) - \frac{g(r)}{r\tan\theta}\frac{\partial Y_l^m}{\partial\theta}(\theta,\varphi), \tag{63}$$

$$E_{\varphi\varphi}^{(1)} = \left[\frac{f(r)}{r} - \frac{m^2}{\sin^2\theta}\frac{g(r)}{r}\right]Y_l^m(\theta,\varphi) + \frac{g(r)}{r\tan\theta}\frac{\partial Y_l^m}{\partial\theta}(\theta,\varphi), \tag{64}$$

$$E_{r\theta}^{(1)} = \frac{1}{2}\left[\frac{f(r)}{r} + \frac{\partial g(r)}{\partial r} - \frac{g(r)}{r}\right]\frac{\partial Y_l^m}{\partial\theta}(\theta,\varphi), \tag{65}$$

$$E_{r\varphi}^{(1)} = \frac{im}{2\sin\theta}\left[\frac{f(r)}{r} + \frac{\partial g(r)}{\partial r} - \frac{g(r)}{r}\right]Y_l^m(\theta,\varphi), \tag{66}$$

$$E_{\theta\varphi}^{(1)} = -\frac{im}{\tan\theta\sin\theta}\frac{g(r)}{r}Y_l^m(\theta,\varphi) + \frac{im}{\sin\theta}\frac{g(r)}{r}\frac{\partial Y_l^m}{\partial\theta}(\theta,\varphi). \tag{67}$$

The stress tensor is determined by Hooke's law: $T_{ij}^{(1)} = 2\mu E_{ij}^{(1)} + \frac{2\mu\nu}{1-2\nu}E_{kk}^{(1)}\delta_{ij}$, where summation over repeated indices is assumed and $\delta_{ij} = 1$ for $i = j$ and 0 for $i \neq j$.

References

Akaiwa, N., Thornton, K., Voorhees, P.W., 2001. Large-scale simulations of microstructural evolution in elastically stressed solids. J. Comput. Phys. 173 (1), 61–86.

Asaro, R.J., Tiller, W.A., 1972. Interface morphology development during stress corrosion cracking: Part I. via surface diffusion. Metall. Trans. 3, 1789–1796.
Ben-Amar, M., Goriely, A., 2005. Growth and instability in elastic tissues. J. Mech. Phys. Solids 53, 2284–2319.
Berger, P., Kohlert, P., Kassner, K., Misbah, C., 2003. Pattern selection in biaxially stressed solids. Phys. Rev. Lett. 90 (17), 176103.
Boley, B.A., Weiner, J.H., 1960. Theory of Thermal Stresses. Wiley, New York.
Cantat, I., Kassner, K., Misbah, C., Müller-Krumbhaar, H., 1998. Directional solidification under stress. Phys. Rev. E 58, 1063651.
Caroli, B., Caroli, C., Roulet, B., Voorhees, P.W., 1989. Effect of elastic stresses on the morphological stability of a solid sphere growing from a supersaturated melt. Acta Mater. 37 (1), 257–268.
Chiu, C., Gao, H., 1993. Stress singularities along a cycloid rough surface. Int. J. Solids Struct. 30, 2983–3012.
Colin, J., Grilhé, J., Junqua, N., 1997. Morphological instabilities of a stressed pore channel. Acta Mater. 45 (9), 3835–3841.
Freund, L.B., Jonsdottir, F., 1993. Instability of a biaxially stressed thin film on a substrate due to material diffusion over its free surface. J. Mech. Phys. Solids 41, 1245–1264.
Grilhé, J., 1993. Study of roughness formation induced by homogeneous stress at the free surfaces of solids. Acta Metall. 41 (3), 909–913.
Grinfeld, M., 1993. Thermodynamics Methods in the Theory of Heterogeneous System. Longman, Sussex.
Haataja, M., Müller, J., Rutenberg, A.D., Grant, M., 2002. Dislocations and morphological instabilities: continuum modeling of misfitting heteroepitaxial films. Phys. Rev. B 65, 165414.
Jou, H.J., Leo, P.H., Lowengrub, J.S., 1997. Microstructural evolution in inhomogeneous elastic media. J. Comput. Phys. 131 (1), 109–148.
Kassner, K., Misbah, C., 1994. Nonlinear evolution of a uniaxially stressed solid: a route to fracture? Europhys. Lett. 28 (4), 245–250.
Kirill, D.J., Davis, S.H., Mikisis, M.J., Voorhees, P.W., 1999. Morphological instability of a whisker. Proc. Royal Soc. London A 455 (1990), 3825–3844.
Kirill, D.J., Davis, S.H., Mikisis, M.J., Voorhees, P.W., 2002. Morphological instability of pores and tubules. Interf. Free Boundaries 4, 371–394.
Larché, F.C., Cahn, J.W., 1985. The interactions of composition and stress in crystalline solids. Acta Metall. 33 (3), 331–357.
Leo, P.H., Sekerka, R.F., 1989. The effect of surface stress on crystal-melt and crystal–crystal equilibrium. Acta Metall. 37 (12), 3119–3138.
Leo, P.H., Iwan, J., Alexander, D., Serkerka, R.K., 1985. Elastic fields about a perturbed spherical inclusion. Acta Metall. 33 (6), 9785–9989.
Leo, P.H., Lowengrub, J.S., Nie, Q., 2000. Microstructural evolution in orthotropic elastic media. J. Comput. Phys. 157 (1), 44–88.
Li, X., Lowengrub, J., Cristini, V., Leo, P.H., 2003. Microstructure evolution in three-dimensional inhomogeneous elastic media. Metall. Mater. Trans. A 34 (7), 1421–1431.
Li, J.H., Stokes, D.W., Caha, O., Ammu, S.L., Bai, J., Bassler, K.E., Moss, S.C., 2005. Morphological instability in InAs/GaSb superlattices due to interfacial bonds. Phys. Rev. Lett. 95, 096104.
Mullins, W.W., 1957. Theory of thermal grooving. J. Appl. Phys. 28, 333–339.
Mullins, W.W., Sekerka, R.F., 1963. Morphological stability of a particle growing by diffusion or heat flow. J. Appl. Phys. 34, 323–329.
Nichols, F.A., Mullins, W.W., 1965. Surface (interface) and volume diffusion contributions to morphological changes driven by capillarity. Trans. Metall. Soc. AIME 233, 1840–1848.
Nozières, P., 1993. Amplitude expansion for the Grinfeld instability due to uniaxial stress at a solid surface. J. Phys. I 3, 681–686.
Ogden, R.W., 1984. Non-linear Elastic Deformation. Dover, New York.
Schöchlin, J., Bohnen, K.P., Ho, K.M., 1995. Structure and dynamics at the Al(1 1 1)-surface. Surf. Sci. (324), 113–121.
Spencer, B.J., Meiron, D.I., 1994. Nonlinear evolution of the stress driven morphological instability in a two dimensional semi-infinite solid. Acta Metall. 42 (11), 3629–3641.
Spencer, B.J., Voorhees, P.W., Davis, S.H., 1991. Morphological instability in epitaxially strained dislocation-free solid films. Phys. Rev. lett. 67 (26), 3696–3699.
Spencer, B.J., Voorhees, P.W., Davis, S.H., 1993. Morphological instability in epitaxially strained dislocation-free solid films: linear stability theory. J. Appl. Phys. 73 (10), 4955–4970.
Srolovitz, D.J., 1991. On the stability of surfaces of stressed solids. Acta Metall. 37 (2), 621–625.
Sun, B., Suo, Z., Evans, A.G., 1994. Emergence of cracks by mass transport in elastic crystals stressed at high tempreatures. J. Mech. Phys. Solids 42 (11), 1653–1677.
Suo, Z., Wang, W., 1994. Diffusive void bifurcation in stressed solids. J. Appl. Phys. 76 (6), 3410–3421.
Thornton, K., Akaiwa, N., Voorhees, P.W., 2001. Dynamics of late-stage phase separation in crystalline solids. Phys. Rev. Lett. 86 (7), 1259–1262.
Wang, A.S.D., Ertepinar, A., 1972. Stability and vibrations of elastic thick-walled cylindrical and spherical shells subjected to pressure. Int. J. Non-Linear Mech. 7, 539–555.
Wang, W., Suo, Z., 1997. Shape change of a pore in a stressed solid via surface diffusion motivated by surface and elastic energy variation. J. Mech. Phys. Solids 45 (5), 709–729.
Wesolowski, Z., 1967. Stability of an elastic, thick-walled spherical shell loaded by an external pressure. Arch. Mech. Stosow. 19, 3–23.
Yang, W.H., Srolovitz, D.J., 1993. Cracklike surface instabilities in stressed solids. Phys. Rev. Lett. 71 (10), 1593–1596.